Wintertime Boundary Layer Structure in the Grand Canyon

C. DAVID WHITEMAN, SHIYUAN ZHONG, AND XINDI BIAN

Pacific Northwest National Laboratory, Richland, Washington

(Manuscript received 19 May 1997, in final form 5 September 1997)

ABSTRACT

Wintertime temperature profiles in the Grand Canyon exhibit a neutral to isothermal stratification during both daytime and nighttime, with only rare instances of actual temperature inversions. The canyon warms during daytime and cools during nighttime more or less uniformly through the canyon's entire depth. This weak stability and temperature structure evolution differ from other Rocky Mountain valleys, which develop strong nocturnal inversions and exhibit convective and stable boundary layers that grow upward from the valley floor. Mechanisms that may be responsible for the different behavior of the Grand Canyon are discussed, including the possibility that the canyon atmosphere is frequently mixed to near-neutral stratification when cold air drains into the top of the canyon from the nearby snow-covered Kaibab Plateau. Another feature of canyon temperature profiles is the sharp inversions that often form near the canyon rims. These are generally produced when warm air is advected over the canyon in advance of passing synoptic-scale ridges.

Wintertime winds in the main canyon are not classical diurnal along-valley wind systems. Rather, they are driven along the canyon axis by the horizontal synoptic-scale pressure gradient that is superimposed along the canyon's axis by passing synoptic-scale weather disturbances. They may thus bring winds into the canyon from either end at any time of day.

The implications of the observed canyon boundary layer structure for air pollution dispersion are discussed.

1. Introduction

Scenic vistas at Grand Canyon National Park (GCNP) have long been a major tourist attraction for American and international visitors. There has been increasing concern, however, about visibility degradation within the park and the southwestern United States as a whole (Trijonis 1979; Macias et al. 1981; GCVTC 1996). This concern about visibility and air quality has led to several major meteorology and air-quality studies in the Grand Canyon region. The Subregional Cooperative, Electric Utility, National Park Service, and Environmental Protection Agency Study (SCENES) Experiment of 1984–89 (Mueller et al. 1986) was a long-term project involving regular visibility and aerosol measurements at a dozen sites in the region. This long-term experiment was supplemented by several short-term intensive experiments in which special air quality and visibility measurements were made, including the Winter Haze Intensive Tracer Experiment (WHITEX), conducted in January and February of 1987 (Malm et al. 1988). Since SCENES ended, other meteorology and air-quality experiments have been conducted to document the effects of nearby coal-fired power plants on visibility within GCNP. The Winter Visibility Study (WVS), on which this paper is based, was conducted in the winter of 1989–90. This was followed by the January and February 1992 winter intensive period of the Measurement of Haze and Visual Effects (MOHAVE) experiment, which investigated the impact of the Mohave Power Plant in Laughlin, Nevada, on canyon visibility (Watson et al. 1993). In general, meteorological analyses to support visibility studies in the region have focused on synoptic- and regional-scale meteorological influences, and on the long-range transport of pollutants into the Southwest (Davis and Gay 1993; Poulos and Pielke 1994; Stauffer and Seaman 1994). Few studies, however, have focused on the evolution of boundary layer structure inside the Grand Canyon and its potential influence on canyon visibility or air quality.

The first observations of vertical temperature structure and winds inside the Grand Canyon were made by research aircraft flights in September and October of 1984 and June of 1985 (Sinclair and Dattore 1987; Stearns 1987). Vertical and horizontal aircraft flight profiles were made during the daytime. The data revealed that winds inside the canyon, which were frequently turbulent, were typically from the southwest (up canyon) and that strong turbulent interactions occurred near the canyon rims between the canyon circulations and the mesoscale flows above the canyon. The data showed

Corresponding author address: C. David Whiteman, K9-30, Battelle Northwest Laboratories, P.O. Box 999, Richland, Washington 99352.
E-mail: Dave.Whiteman@pnl.gov

that daytime heating in the canyon was asymmetric, with the south-facing walls warming much more quickly than the north-facing walls, and that daytime temperature lapse rates in the canyon were essentially dry adiabatic. The dataset, unfortunately, provided no wintertime or nighttime descriptions of temperature and wind patterns inside the canyon.

The Winter Visibility Study of 1989–90 was conducted to determine the contribution to visibility impairment at GCNP from the Navajo Generating Station, a coal-fired power plant located at Page, Arizona, and to estimate the visibility improvement that would occur with emission reductions (Richards et al. 1991; Lindsey et al. 1999). As part of the field program, wind and temperature profiles were made using balloon sonde, tethered balloon, and radar profiler observations from the floor of the Grand Canyon at Phantom Ranch, Arizona. A scanning Doppler lidar was also operated from the south rim of the Grand Canyon at Hopi Point (Gaynor and Banta 1991; Banta et al. 1999). Lidar analyses showed that strong stable layers at rim level act to decouple the flow within the canyon from the overlying cross-canyon ambient flows. When the stability is weak, ambient flows can penetrate into the upper canyon. Further, when ambient flows above the canyon are weak, a down-canyon jet may enter the canyon from Marble Canyon to the north. This flow is strongest at night but may be reversed during daytime (Banta et al. 1991). Flows in the upper half of the canyon may counter the winds below, forming a recirculating or antiwind system.

In this paper, wind and temperature data from WVS soundings are used to investigate the structure and evolution of the boundary layer in the Grand Canyon, to compare the Grand Canyon structure to that of other valleys, to postulate mechanisms that can explain the structural differences, and to anticipate the effects of the structure on canyon air pollution transport and dispersion. The most surprising aspects of the present study are the very fundamental differences between the boundary layer structure in the Grand Canyon and that in other valleys of the western United States.

The paper is organized into seven sections. The site characteristics and data are described in section 2. Section 3 describes the temperature structure evolution within the canyon. Section 4 compares the temperature structure in the Grand Canyon to that of other valleys in the Rocky Mountains. Section 5 discusses the elevated stable layers that are often observed above the canyon. Section 6 discusses the canyon wind field. Conclusions are drawn in section 7.

2. Sites, instrumentation, and data

a. Sites

The WVS experiment was conducted in the Grand Canyon region of Utah, New Mexico, Arizona, and Nevada. Figure 1 shows the locations of selected WVS sites. Detailed information on the sites is given in Table 1.

The Grand Canyon of the Colorado River (Fig. 1) is a deep canyon cutting east to west through an area of high plateaus that marks the western side of the Colorado Plateaus Basin, an elevated basin bounded to the north, east, and south by the Rocky Mountains. The Grand Canyon is the main channel connecting the Colorado Plateaus Basin to the lower-lying Basin and Range Province, a region of short north–south mountain ranges separated by broad basins that extends through the Great Basin from eastern Oregon through Utah and Nevada into Texas. The lower-lying areas within the region are semiarid or arid and are composed largely of exposed desert soils and rock, while the higher elevations receive enough precipitation to support extensive evergreen forests, and are covered with snow in winter.

High plateaus are located to the north and south of the Grand Canyon. The Coconino Plateau south of the canyon slopes gently upward to the north to form the canyon's south rim (Fig. 2). Farther northward, the canyon drops away steeply (22°) to the Colorado River and the Phantom Ranch site where upper-air soundings were launched in the WVS experiment. Phantom Ranch is located on the floor of the Grand Canyon where the Bright Angel Canyon enters the westward-flowing Colorado River from the north. In the vicinity of Phantom Ranch, the main canyon contains a V-shaped ''inner canyon,'' but widens abruptly above the inner canyon at an elevation of around 1100 m above mean sea level (MSL). Continuing northward from the river, the canyon walls rise at an average 6° angle through a series of eroded terrain projections termed towers, thrones, temples, etc. (Hamblin and Murphy 1980) to the canyon's north rim. The north rim is the edge of the Kaibab Plateau, a forested high-elevation plateau with a continuous wintertime snow cover. The canyon's south and north rims have elevations near 2150 and 2450 m MSL, respectively.

b. Instrumentation

Upper-air soundings from the Phantom Ranch site were made by the National Oceanic and Atmospheric Administration's Environmental Technology Laboratory (formerly the Wave Propagation Laboratory) using tethered and free-flying balloon sounding systems manufactured by Atmospheric Instrumentation Research, Inc., of Boulder, Colorado. The tethered balloon sounding system (Tethersonde) collected pressure, temperature, humidity, and wind data at 10-s intervals in soundings that typically attained 2000 m MSL in continuous ascents lasting about 35 min. This sounding system has precisions of ± 1 mb for pressure, ± 0.5°C for the dry and wet bulb temperature sensors, $\pm 5\%$ for humidity, ± 0.25 m s^{-1} for wind speed, and ± 5 deg for wind direction. The free-flying balloon sondes (Airsondes)

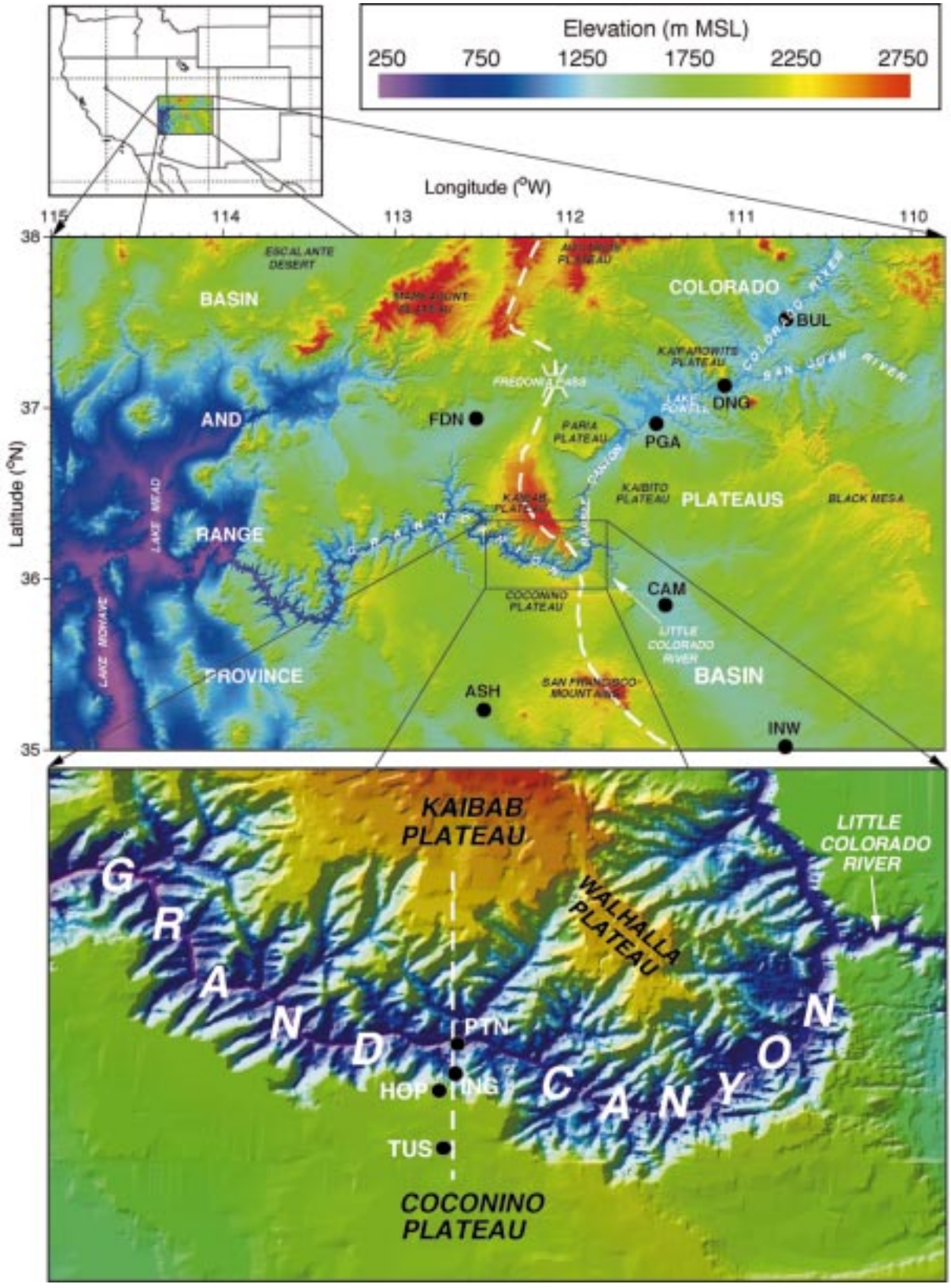

FIG. 1. Shaded relief map of the Grand Canyon region from three-arc-second gridded elevation data. Key topographic features are labeled and selected meteorological sites are shown as dots (cf. Table 1). North is at the top of the figure; the height legend is in meters MSL. The lower panel is a close-up of the shaded relief map in the vicinity of Phantom Ranch. The dashed line indicates the location of the cross section in Fig. 2.

TABLE 1. Locations of surface and upper-air stations mentioned in the text. The types of data used in our analyses are shown in the last column. Other types of data are available at many of these sites.

Site name	Ident	Latitude	Longitude	Altitude (m MSL)	Data type*
Ash Fork	ASH	35°14′21″	112°29′00″	1588	RS
Bullfrog Basin	BUL	37°31′08″	110°43′30″	1130	RS
Cameron	CAM	35°50′54″	111°25′39″	1350	RS
Dangling Rope	DNG	37°07′48″	111°04′53″	1155	RS
Fredonia	FDN	36°56′17″	112°31′46″	1420	Sodar
Hopi Point	HOP	36°04′16″	112°09′14″	2152	SFC
Indian Garden	ING	36°04′45″	112°07′37″	1146	SFC
Page	PGA	36°54′47″	111°28′45″	1332	AS
Phantom Ranch	PTN	36°06′55″	112°03′34″	750	AS & TS
Tusayan	TUS	35°57′	112°09′	2012	RS
Winslow	INW	35°01′	110°44′	1488	RS

* RS = rawinsonde, SFC = surface meteorology station, AS = airsonde, TS = tethersonde.

ascended through the canyon atmosphere at rates of about 200–250 m min^{-1}, providing pressure, temperature, and humidity data at height intervals of about 50 m, with published precisions of ±3 mb for pressure (accuracy is improved by adjusting the indicated pressure to a reference standard before launch), ±0.5°C for dry and wet bulb temperature, and ±3% for humidity. The free-flying sondes were not tracked to determine winds.

c. Data

The WVS experiment began on 12 January and ended on 3 March 1990. During this period, tethered balloon and airsonde soundings were made at irregular time intervals at the Phantom Ranch site. Equipment and supplies were ferried to the site by helicopter and mule before and during the experiment, and observers hiked into and out of the canyon during winter conditions to occupy the Phantom Ranch site and make the soundings.

Before discussing the data analyses, it is important to state the analysis limitations. The original experimental design called for continuous radar profiler wind observations from Phantom Ranch along with regular and frequent tethered balloon soundings of wind and temperature structure. Airsondes were to be used as backups when winds or other conditions precluded tethered balloon ascents. Shortly after the site was commissioned, however, tethered balloon flight restrictions were imposed by the National Park Service for reasons of aircraft flight safety because an emergency helicopter landing facility was in the neighborhood of the Phantom Ranch site. This resulted in a decision to fly tethered balloons only at night and to fly airsondes during daytime. The airsondes were not optically tracked to determine winds, since winds were sensed continuously by the Phantom Ranch radar profiler. Unfortunately, post-experiment analyses of the radar profiler wind data showed contamination by radar beam reflections from the canyon sidewalls, so that data below 500–600 m above ground level (AGL) were deemed unusable. Radar profiler winds in the upper portion of the canyon were also inconsistent with selected tethered balloon wind soundings, so that these radar profiler data are also suspect. Wind data in the canyon are, therefore, limited to the nighttime tethered balloon ascents. Temperature and humidity structure data from the tethered balloon and airsonde ascents are, however, available during all hours of the day and night.

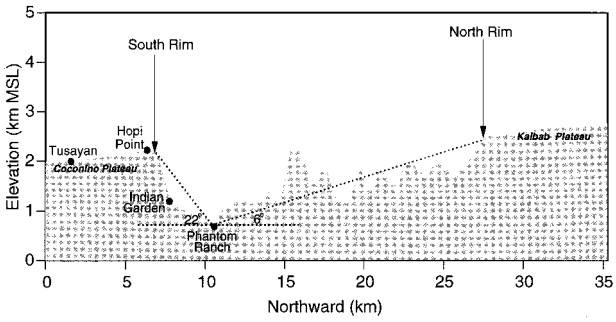

FIG. 2. North–south vertical cross section across the Grand Canyon through the Phantom Ranch site at the location shown by the dashed line in Fig. 1.

3. Temperature structure and its evolution in the Grand Canyon

Canyon temperature structure was determined from 57 nighttime tethered balloon soundings and 86 airsonde soundings (84 during daytime and 2 during nighttime) from Phantom Ranch.

a. Afternoon temperature soundings

Twenty-five afternoon temperature soundings (22 at around 1600 and 3 at around 1300 mountain standard time, MST) are plotted in Fig. 3 for individual days of the experiment to illustrate the range of afternoon temperature profiles within and above the canyon. The weather was quite variable during the 25 days, ranging from clear days with light winds to cloudy days with

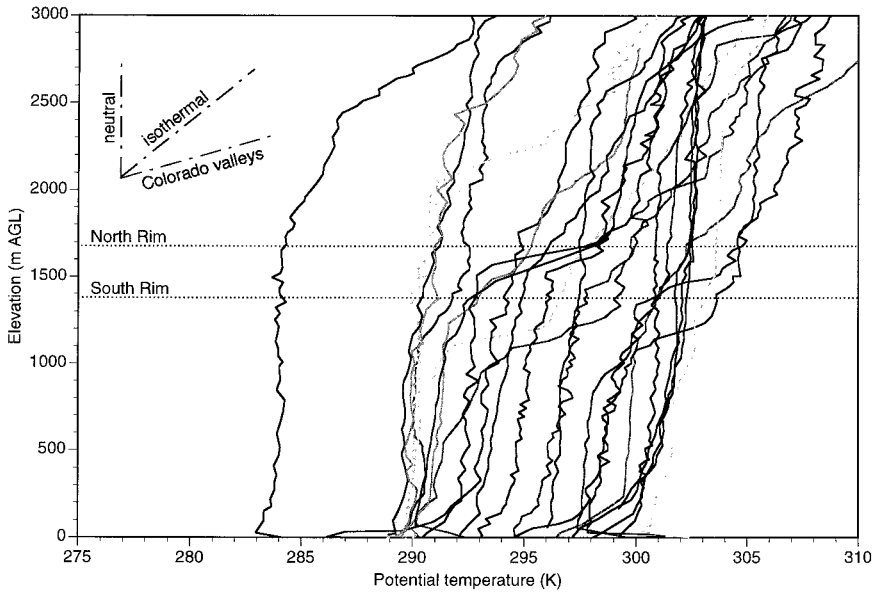

FIG. 3. Late afternoon (~1600 MST) potential temperature soundings from the floor of the Grand Canyon at Phantom Ranch. The approximate heights of the canyon's north and south rims are indicated. Neutral and isothermal potential temperature gradients are indicated for comparison, as well as the mean near-sunrise potential temperature gradient (0.030 K m^{-1}) for Colorado valleys (first 14 entries in Table 2).

stronger winds and precipitation. Potential temperatures within the canyon varied from 283 to 305 K during these days, but the midcanyon atmosphere consistently exhibited a near-neutral temperature profile. At the surface, superadiabatic sublayers were present on some days, while shallow stable layers were present on other days. On approximately seven of the afternoons the canyon neutral layer was capped by strong potential temperature jumps. These jumps, which occurred in the canyon profiles at elevations near the canyon rims, will be discussed in section 5.

b. Morning temperature soundings

Forty-one temperature soundings were collected on separate mornings during the experimental period. Of these, 37 were launched between 0555 and 0738, and four were launched around 1000 MST. Sunrise times varied from 0744 to 0658 MST during this period.

These morning potential temperature profiles could be classified into two categories. The first category, containing 23 soundings, had near-neutral profiles (Fig. 4). The mean potential temperature gradient within the canyon in these soundings was about $d\theta/dz = 0.002$ K m^{-1}. Most soundings had a stable sublayer in the lowest 50 m. Like the afternoon soundings, some of the morning neutral stability soundings exhibited potential temperature jumps near the canyon rims. Some tethered balloon soundings were terminated before reaching the canyon rims because of winds that exceeded the operational limits of the tethered balloon system.

The second category, containing 18 soundings, exhibited stronger stabilities (Fig. 5). The mean midcanyon potential temperature gradient in these soundings was $d\theta/dz = 0.008$ K m^{-1} (i.e., $dT/dz = -0.0018$°C m^{-1}). This temperature gradient is slightly less stable than isothermal. As for the near-neutral morning soundings, the near-isothermal soundings often had a stronger stability surface layer in the lowest 50 m. One or two of these soundings exhibited a potential temperature jump near the elevation of the canyon rims. A surprising feature of the near-isothermal soundings is the general lack of a sharp discontinuity at rim level between the potential temperature gradients within and above the Grand Canyon.

c. Temperature structure evolution

The afternoon and early morning soundings in Figs. 3–5 represent 66 of the 143 available soundings. The remaining soundings were mostly multiple soundings made on individual days to document canyon temperature structure evolution. The canyon's diurnal temperature structure evolution followed two basic patterns, illustrated in Figs. 6 and 7. In the first pattern (Fig. 6), the canyon underwent warming and cooling while maintaining a near-neutral stratification. In the 20 January 1990 example, the diurnal cycle had an amplitude of 5 K through essentially the entire canyon depth. This type of temperature structure evolution, which occurred under various synoptic conditions, was frequently observed. In the second type of temperature structure evolution (Fig. 7), the diurnal potential temperature range was largest near the canyon floor and became smaller

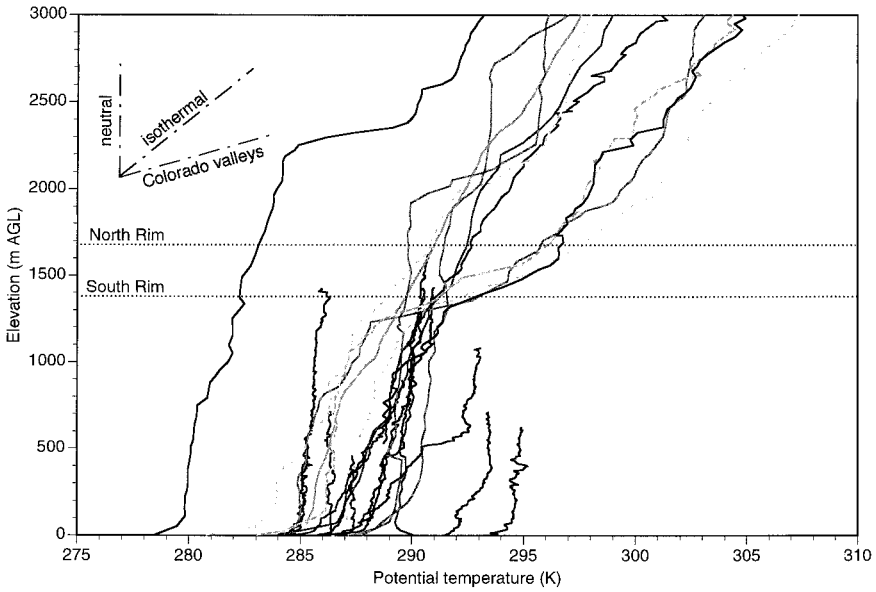

FIG. 4. Same as Fig. 3, but for near-neutral early morning (~0630 MST) potential temperature soundings.

as the rim level was approached. The potential temperature gradient was near-neutral during afternoon, but the larger diurnal change near the canyon's floor produced a more stable temperature structure within the canyon at night than was experienced with the first type of temperature structure evolution. This second pattern of deep nighttime stabilization/daytime destabilization occurred when skies were clear and winds aloft were weak—conditions normally associated, in other valleys, with the development of strong temperature inversions that form over the valley floor and grow in depth during the night. In both types of temperature profile evolution the heating and cooling occurred through almost the entire canyon depth, rather than being limited to a shallow layer near the canyon floor.

4. Comparison of Grand Canyon temperature structure with other valleys

In other Rocky Mountain valleys, the continuous upward growth of a stable boundary layer from the valley floor is a key nighttime feature of temperature structure

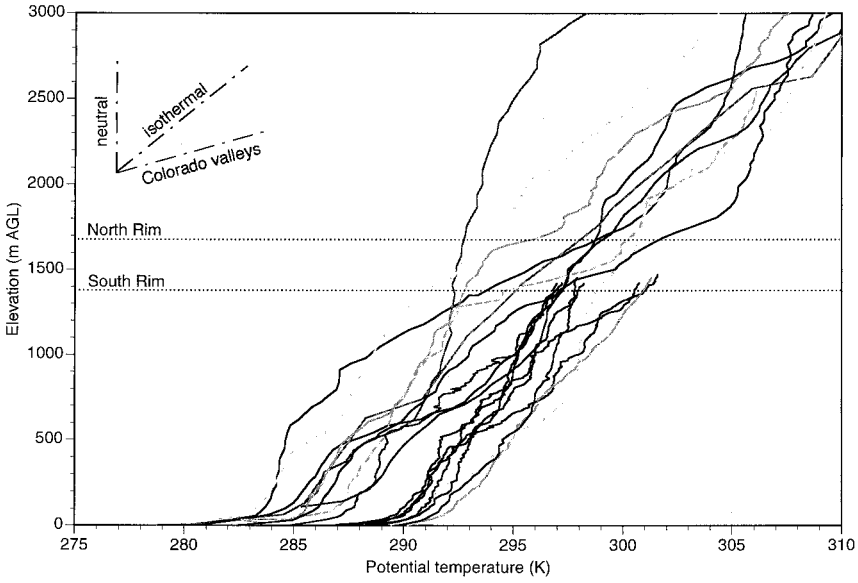

FIG. 5. Same as Fig. 3, but for near-isothermal early morning (~0630 MST) potential temperature soundings.

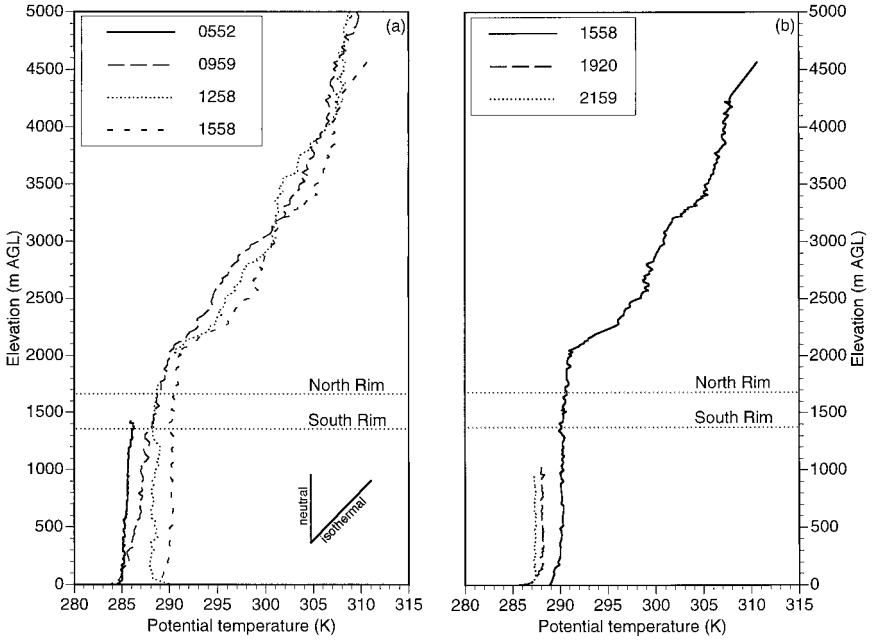

FIG. 6. First pattern of temperature structure evolution within the Grand Canyon, in which diurnal warming and cooling occurs while maintaining a near-neutral stratification. Phantom Ranch, 20 January 1990, during the (a) warming and (b) cooling periods. Times indicated are in MST.

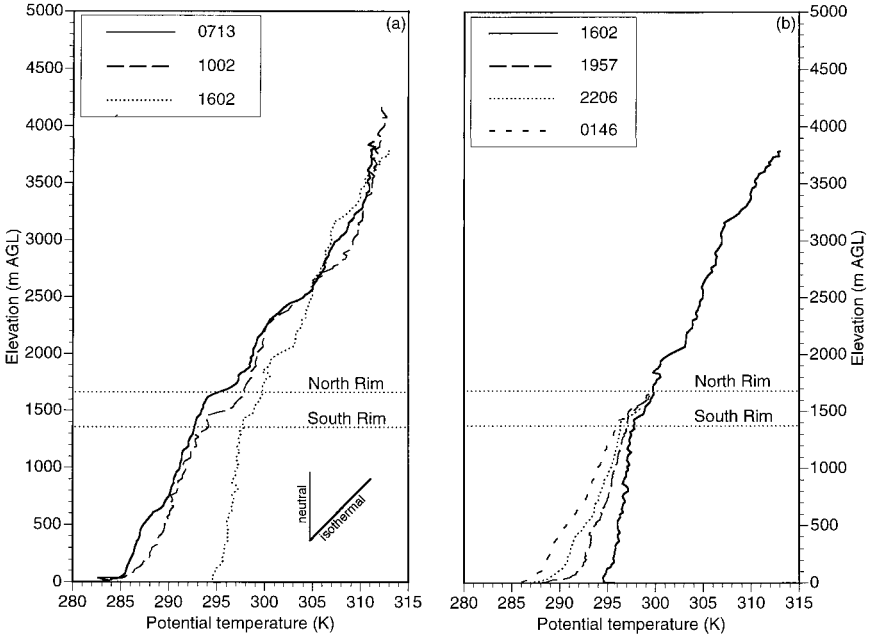

FIG. 7. Second pattern of temperature structure evolution within the Grand Canyon, in which the profiles destabilize during daytime and stabilize during nighttime through the whole valley depth. Phantom Ranch, 22–23 February 1990, during the (a) warming and (b) cooling periods. Times indicated are in MST.

TABLE 2. Near-sunrise stable boundary layer characteristics after clear nights with light wind speeds aloft.

No.	Location[a]	Date	Valley depth (m)	Inversion depth (m)	Inversion strength (K)	Potential temperature gradient (K m^{-1})	Morning heat deficit (MJ m^{-2})
	Eagle Valley						
1	Ray Miller residence, Eagle-Vail, CO	13 Oct 1977	700	675	17.9	0.027	6.1
2	Steve Miller residence, Eagle-Vail, CO	12 Oct 1977	700	585	15.3	0.026	4.5
	Yampa Valley						
3	Horseshoeing School, Steamboat Springs, CO	10 Aug 1978	450	535	17.5	0.033	4.7
4	Sombrero Stables, Steamboat Springs, CO[b]	22 Feb 1978	450	438	24.3	0.056	5.3
	White River Valley, South Fork						
5	Mobley Ranch, CO	27 Aug 1978	350	585	20.1	0.034	5.9
6	Sleepy Cat Guest Ranch, CO	29 Aug 1978	300	525	17.8	0.034	4.7
7	Stillwater, CO	24 Aug 1978	750	291	8.4	0.029	1.2
	Roaring Fork Valley						
8	North Star Ranch, Aspen, CO	19 Jul 1978	750	640	14.5	0.023	4.7
	Gunnison Valley, North Fork						
9	Rol Holt residence, Paonia, CO	21 Jul 1978	800	414	10.2	0.025	2.1
	Poudre Valley						
10	Poudre River Trout Hatchery, CO	14 Jul 1978	600	425	9.0	0.021	1.9
	Gore Valley						
11	Golf Course, Vail, CO[b]	18 Oct 1975	650	670	22.7	0.034	7.6
12	Municipal Building, Vail, CO	6 Jul 1978	700	750	17.5	0.023	6.6
13	Safeway Store, Vail, CO[b]	10 Oct 1975	600	450	16.9	0.038	3.8
	Corral Gulch						
14	Piceance Basin, Oil Shale Tract C-a, CO	typical Aug	105	256	11.9	0.047	1.5
	Colorado Valley						
15	Airport, Grand Junction, CO	mean	—	198	6.7	0.034	0.7
16	Ash Fork, AZ[c]	12 Jan 1990	546	346	15.6	0.045	2.7
17	Bullfrog Basin, UT[c]	12 Jan 1990	1004	1342	19.7	0.015	13.3
18	Cameron, AZ[c]	12 Jan 1990	784	852	19.3	0.023	8.3
19	Dangling Rope, UT[c]	12 Jan 1990	979	1439	17.0	0.012	12.3
20	Phantom Ranch, AZ[c]	typical, Fig. 5	1384	1384	10.5	0.008	7.3

[a] Data for 1–13 and 15 from Whiteman (1980), 14 from Whiteman et al. (1981).
[b] Snowcover was present.
[c] Elevation of south rim (2134 m MSL) was used to calculate valley depth.

evolution. This stable boundary layer growth has been shown by previous investigators for a small basin (Whiteman et al. 1996, Fig. 6), for a midsized valley (Whiteman 1986, Fig. 1), and for a small valley (Doran et al. 1990, Fig. 2). The stable layer growth is produced by the convergence of cold downslope flows over the valley center, and the subsequent buildup of a cold air layer within the valley. Similarly, growing convective boundary layers are a typical feature of valley temperature structure evolution during daytime (Whiteman 1982). These boundary layers grow over the heated valley floor and sidewalls after sunrise as they erode the elevated base of the remnant of the nocturnal valley temperature inversion, eventually destroying the nocturnal inversion and coupling the valley atmosphere to the atmosphere above the valley. Surprisingly, the Phantom Ranch soundings do not show either the typical nighttime stable boundary layer growth or the typical daytime unstable boundary layer growth within the canyon that is characteristic of other valleys.

While stabilities are weak in the Phantom Ranch soundings, they are expressed over deep layers. Other valleys (Table 2), in contrast, have strong stabilities expressed over shallower layers. Because depth and strength of the morning stable layer vary from valley to valley, an appropriate way of intercomparing valley energetics is to compare their morning heat deficits. The morning heat deficit is the amount of heat required to break the nocturnal inversion. It can be determined from a single sounding obtained near sunrise following a clear undisturbed night by calculating the heat required to convert the morning sounding to a constant potential temperature sounding having the potential temperature observed at the top of the ground-based stable layer. This heat deficit D is proportional to the product of inversion depth and strength, and can be approximated by

$$D = 0.5\rho c_p H \Delta\theta \quad [\text{J m}^{-2}], \tag{1}$$

where H is inversion depth, $\Delta\theta$ is inversion strength, ρ is air density, and c_p is the specific heat of air at constant pressure. The morning heat deficits are thus proportional to the triangular areas obtained by connecting the origin to the individual points in Fig. 8 and dropping a vertical line to the abscissa. The energy deficits range from 0.7 MJ m^{-2} at Grand Junction to 13.3 MJ m^{-2} at Bullfrog Basin (Table 2). The heat deficit at Phantom Ranch is 7.3 MJ m^{-2}, a value comparable to, but slightly larger

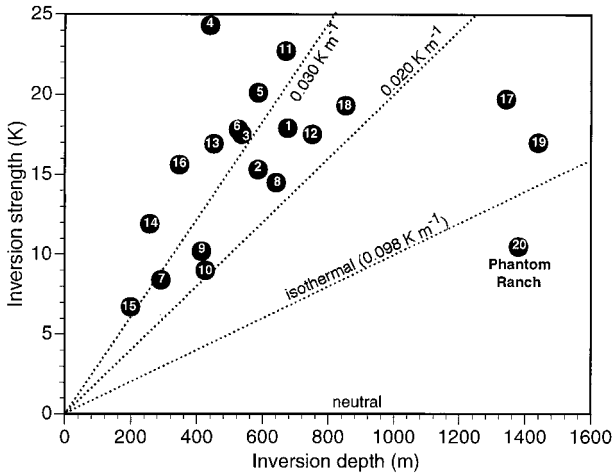

FIG. 8. Potential temperature difference between the ground and the top of the nocturnal inversion vs inversion depth for valleys, basins, canyons, and plains locations in the central and southern Rockies. Data from Table 2.

than, heat deficits in many midsized Colorado valleys (4–7 MJ m^{-2}).

The morning heat deficit must be overcome by daytime heat flux convergence if the nighttime stable layer is to be destroyed diurnally. The morning heat deficit in valleys, basins, and other low-lying areas is greatly enhanced by the nighttime drainage of cold air off the higher terrain. The heat deficit above a low-lying point within an airshed is, therefore, dependent on the amount of sensible heat lost from the airshed drainage area as well as the detailed topography of the airshed, which governs the locations and characteristics of the cold air pools. This nighttime convergence of cold air over low-lying areas is largely responsible for the high heat deficits found at valley and basin sites. The morning heat deficit over the plains at Grand Junction, 0.7 MJ m^{-2}, if built up steadily over a 12-h night, would require heat loss at the rate of 16 W m^{-2}. Over Bullfrog Basin, a site in the lowest-lying terrain of the Colorado Plateaus Basin, the corresponding calculated rate of heat loss is 308 W m^{-2}, a value much larger than could be supported by local surface energy budget processes. At Phantom Ranch, the rate of heat loss is 169 W m^{-2}. This rate of loss is, no doubt, produced by cold air convergence into the canyon, especially from the snow-covered Kaibab Plateau north of the canyon. In the case of the Bullfrog Basin and Dangling Rope sites northeast of the canyon, the carryover of atmospheric heat deficits from day to day plays a role in producing the large calculated heat deficits (Whiteman et al. 1999b). In the case of the Phantom Ranch site, however, daytime soundings are neutral so that no heat deficit carryover occurs from day to day. Further, the largest morning heat deficits within the canyon, which occur with isothermal profiles, do not vary significantly between nights in which canyon winds are up- or down-valley, suggesting that cold air convergence within the canyon comes primarily from local cross-valley convergences rather than being produced by along-canyon advection.

The comparison of nighttime heat deficits in various valleys shows that the weak stabilities within the Grand Canyon are not due to weaker cooling in the canyon, but rather to the distribution of the nighttime cooling through a deeper layer. This deeper distribution of the cooling results in weak stabilities that will have important implications for air pollution dispersion in the canyon, since both vertical and horizontal dispersion become larger as stability decreases. Stability in the Grand Canyon, as measured near sunrise following clear undisturbed nights, is 0.006–0.010 K m^{-1}, considerably lower than in nearby valleys or basins, in other valleys on the west side of the central and southern Rockies, and over the nearby plains (Table 2 and Fig. 8). At the Bullfrog Basin and Dangling Rope sites upstream of the canyon in the Colorado Plateaus Basin, potential temperature gradients are typically 0.012 and 0.015 K m^{-1}, respectively. In the central and southern Rockies average potential temperature gradients are 0.030 K m^{-1} (average of entries 1–14 in Table 2). Finally, at Grand Junction, Colorado, on the western edge of the Rockies, inversions are shallow (~200 m deep), and potential temperature gradients are strong (0.034 K m^{-1}). Morning soundings at Denver, Colorado, on the eastern edge of the Rockies, have inversion characteristics similar to those at Grand Junction (Holzworth and Fisher 1979). A key question raised by the observations, then, is why the Grand Canyon exhibits such weak morning stability compared to other valleys and basins and what mechanisms could be responsible for distributing the nighttime cooling over the entire canyon depth. These questions will be addressed below in the form of hypotheses and, where data are available, the evidence supporting or rejecting individual hypotheses will be stated.

The first hypothesis is that weak nighttime stabilities in the canyon are produced by advection of weak stability air into the canyon from either end. This hypothesis can be rejected because canyon potential temperature gradients are generally more neutral than gradients upstream (sites 17–19 in Table 2) or downstream (site 16 in Table 2) of the canyon.

A second hypothesis is that weak stabilities in the Grand Canyon are produced by cloud cover. This hypothesis can be rejected as an explanation for the stability differences between the canyon and other valleys because the canyon is not always cloudy, and canyon stabilities are weak even when cloud cover is absent. Cloud cover, however, may explain differences in canyon stability from night to night. Cloud cover is expected to reduce nighttime radiational cooling, leading to radiative interactions between the valley floor, sidewalls, and cloud base, and driving the canyon atmosphere toward radiative equilibrium and isothermalcy. To examine the effect of clouds, a ''clearness index'' was devised by calculating the ratio of daytime-inte-

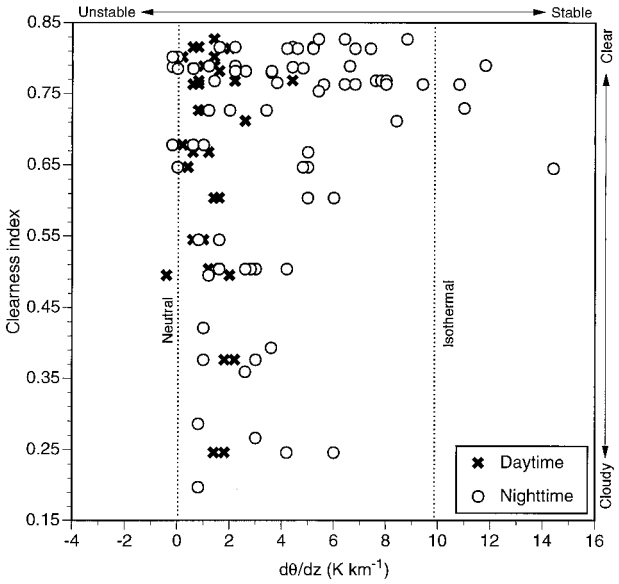

FIG. 9. Main canyon stability vs the clearness index.

grated incoming solar radiation at Hopi Point, 6 km southwest of Phantom Ranch on the canyon's south rim, to daytime-integrated extraterrestrial solar radiation (i.e., the radiation incident at the edge of the earth's atmosphere before attenuation by the atmosphere) as calculated by Whiteman and Allwine's (1986) solar model. A ratio of 0.7 or more is indicative of clear skies, a ratio below 0.2 indicates cloudy skies, and intermediate values indicate partially cloudy skies. Figure 9 shows the relationship between the clearness index and the average stability in the main canyon, as measured by the potential temperature gradient above Phantom Ranch between 500 and 1000 m above ground level. The daytime points are clustered near neutral stratification, regardless of cloudiness; nighttime points are scattered between neutral and isothermal. The stronger stability soundings occur with clear nighttime skies, but only 4 of the 74 nighttime soundings exhibit stabilities greater than isothermal. Weak stability soundings, however, appear under both clear and cloudy conditions. Thus, the occurrence of near-neutral stabilities in the canyon bears little relationship to cloudiness. Further, the establishment of a radiative equilibrium in the canyon due to cloud cover is apparently not the main factor producing isothermal profiles within the canyon since, as Fig. 9 shows, isothermal profiles tend to occur during clear nights rather than during cloudy nights.

A third hypothesis is that other radiative effects (besides those associated with clouds) are responsible for the weak stabilities in the canyon. These processes will be discussed for both daytime and nighttime.

During the day, the receipt of downward shortwave radiation in the canyon is limited by shadows that are cast into the canyon by the south rim. While the steep south-facing slope receives significant amounts of solar radiation because of its favorable slope and aspect angles, the steep north-facing slope receives little or no direct solar radiation on midwinter days. The Indian Garden site on the south wall of the Grand Canyon receives direct radiation for only a few hours in the early afternoon during winter. The Phantom Ranch site on the canyon floor also is in shadow much of the day and receives direct solar radiation only during a 3.5-h period in midday (Ruffieux 1992) during winter, which explains the slightly stable surface layer found in several of the afternoon soundings in Fig. 3. A shallow superadiabatic sublayer appears at this site only during the period when the sun is shining directly on the site (see the 1258 MST sounding in Fig. 6), so that the neutral layer above Phantom Ranch that persists during the entire day cannot be attributed to convection from the canyon floor, but is rather a consequence of the distribution of heat across the valley cross section caused by differential insolation on the opposing sidewalls. The strong receipt of solar radiation on the south-facing sidewall will lead to convective boundary layers, up-slope flows, vertical mixing, and cross-valley circulations, and the canyon atmosphere as a whole must be warmed by the resulting circulations. No direct observations of the warming of the south-facing sidewall were collected as part of the WVS, but Stearns (1987) observed rapid warming on the south-facing sidewall using airborne infrared radiometers.

At night, the canyon atmosphere may be destabilized by radiative flux divergence that increases with elevation. This increase often occurs in valley or canyon atmospheres since downward radiative flux increases with depth in the canyon due to the increase of solid angle of the relatively warm radiating sidewalls and the decrease of the solid angle of the cold radiating sky. Ruffieux (1992) presents measurements of net all-wave radiation at Hopi Point and Phantom Ranch on the clear night of 16 January 1992 to illustrate this increase of net radiative loss with elevation. Petkovsek (1978) provides a formula to determine the influence of sidewall steepness on the sky-view factor, that is, the openness of the horizon within a canyon. In the case of the Grand Canyon, the south and north slopes have mean slope angles of 22° and 6°, which would reduce the sky-view factor at the canyon floor by 16% compared to a plain. The view of the sky improves with distance up the sidewalls, so that downward radiative flux decreases with distance up the slope (in actuality, the sky view factor would vary significantly within the canyon because of the rough terrain and vertical cliffs). The effect of the sky-view factor on nighttime radiative cooling is supported by Ruffieux and Whiteman's (1991) study of wintertime surface energy budgets in the Grand Canyon region. They found that downward longwave radiative flux is significantly increased in the lower elevations of the canyon by the warm radiating sidewalls. The existence of a vertical gradient of net radiative flux divergence in the canyon will destabilize the canyon atmo-

sphere by preferentially cooling the upper-canyon atmosphere. This factor alone, however, seems unlikely as an explanation for weak stabilities in the canyon, as many other valleys (e.g., Colorado's Brush Creek Valley) have similar average sidewall angles yet maintain stronger stabilities.

A fourth hypothesis is that canyon stabilities are reduced by strong winds that produce mechanical mixing within the canyon. Start et al. (1975) offered this explanation for enhanced diffusion in Huntington Canyon (they presented no information on measured stabilities, however). They proposed that the enhanced diffusion there was due to turbulence generated by strong winds at mountaintop level that penetrates into the valley, and to wake turbulence produced by strong winds in the lee of canyon terrain obstacles. The Grand Canyon certainly has many internal obstacles and roughness elements. Strong winds, however, cannot explain the stability differences between the Grand Canyon and other valleys since the canyon experiences light wind nights in which the stabilities are also weak. Nonetheless, strong wind events might explain stability differences within the canyon from night to night. To investigate this, tethered balloon wind soundings inside the Grand Canyon were compared to airsonde soundings above the canyon launched from the Coconino Plateau at Tusayan, Arizona. In the few cases when the Tusayan and Phantom Ranch soundings both showed strong winds, the canyon temperature soundings, indeed, had a near-neutral stratification. There were, however, many cases when the canyon winds were weak. Some of these events occurred when above-canyon winds were also weak, and others occurred when stronger winds above the canyon were decoupled from the winds inside the canyon by inversions that formed above the canyon rims. In both cases, the nighttime temperature soundings within the canyon exhibited near-neutral stability. Therefore, strong winds in the canyon appear to be sufficient, but not necessary for the existence of weak stability in the Grand Canyon atmosphere.

A fifth hypothesis is that canyon stabilities are reduced by vertical mixing caused by the formation of a large horizontal-axis eddy within the canyon. Such a mechanism was suggested by Start et al. (1975) to explain enhanced plume diffusion in Huntington Canyon. They suggested that, where the canyon is narrow, downslope flows of cold air from sidewalls or feeder canyons could descend to the valley floor and rise up the opposite slope, producing a large horizontal-axis eddy generating pulses of helical circulations. Such an eddy could mix the canyon atmosphere vertically and would be produced even when the cross-valley flow is weak at the top of the canyon and under stable conditions. Although observational data are limited in the Grand Canyon, this mechanism can be tentatively rejected based on Phantom Ranch surface wind (Whiteman et al. 1999a) and tethered balloon observations that show no strong nighttime winds descending the Bright Angel Canyon or coming off the sidewalls at the top of the inner canyon.

A sixth hypothesis is that the weak canyon stability is produced by overturning and mixing of air within the canyon by the introduction, at rim level, of cold air generated on the high-elevation plateaus north and south of the canyon. The sinking of cold convective plumes, like the daytime rising of warm convective plumes, mixes air vertically, and does not depend on canyon wind strength and direction. The elevated Kaibab and Walhalla Plateaus could provide a prodigious source of cold air, while the Coconino Plateau, which slopes downward to the south away from the canyon rim, would seemingly be a poorer cold air source since much of the air would drain southward away from the canyon rather than into the canyon. Since the plateaus are snow covered in winter, a flow of cold air off the plateaus could occur also during daytime, enhancing the daytime mixing in the canyon caused by upward convection of warm air from the heated canyon sidewalls. The postulated cold airflow off the plateaus is supported by visual observations of smoke from the Vista prescibed fire on the Walhalla Plateau (Fig. 1) in September 1980 (J. W. Ray 1997, personal communication). During that fire, smoke was seen to fall off the rim into the canyon like a waterfall in the late afternoon and evening. The smoke, once it drained into the canyon, became well-dispersed vertically throughout the canyon during the night. Snow cover was not present on the plateau during this fire, which continued to burn for several weeks.

The turbulent mixing of the cold air around the numerous terrain obstacles and vertical cliffs as it descends the canyon sidewalls may be the explanation for the lack of strong coherent downslope flows on the lower sidewalls and the corresponding absence of strong cold air convergence and stable boundary layer growth over the canyon floor. The downward (negative) convection mechanism is appealing as an explanation for the canyon potential temperature profile evolution as it can explain why the cooling and warming occur through the entire canyon depth, rather than through boundary layers that grow upward from the canyon floor during night or day.

Snow cover on the plateaus, no doubt, increases the cold air source strength. Snow cover alone, however, cannot explain the weak stabilities in the canyon, as strong nighttime stabilities have been observed in other snow-covered valleys (Table 2, sites 4, 11, and 13). Rather, the location of the snow-covered plateau cooling surfaces above the canyon rims may be an important factor. Another factor that may decrease the strength of downslope flows in the canyon is the inverse dependence of drainage flow strength on sidewall angle (e.g., Arritt 1985; Petkovsek and Hocevar 1971; Petkovsek 1978). This inverse dependence is, however, controversial and is contradicted by other models (e.g., Nappo and Rao 1987; Atkinson 1995).

We have considered a number of individual hypotheses to explain the weak stabilities in the canyon relative

to other valleys of the Rocky Mountains, but it is likely that a variety of mechanisms that distribute the nighttime cooling through the entire canyon depth act together to produce the weak stabilities. Unfortunately, the available data are insufficient to provide comprehensive tests of even the individual hypotheses. A combination of model simulations and additional meteorological data may be necessary to provide a complete explanation. Our initial simulations with a two-dimensional mesoscale atmospheric dynamic model have been largely unsuccessful. The complexity of the three-dimensional Grand Canyon terrain, the large modeling domain required to include the entire canyon (approximately 450 km long) and its surroundings, and the necessity of resolving shallow drainage flows on the sidewalls imposes extremely stringent computational requirements. Further, such models cannot yet adequately simulate radiative exchange in complex terrain settings and the adequacy of existing turbulence parameterizations is unclear in this steep, complex terrain setting.

5. Elevated stable layers at and above the canyon rims

The generally neutral stratification within the canyon and the cooling and warming through the entire depth of the canyon are two features of the diurnal evolution of temperature structure within the canyon. A third feature of the canyon's temperature structure evolution is the frequent occurrence of potential temperature jumps or stable layers at the top of the canyon. The strong stability of these inversion layers is in contrast to the weak stability of the canyon atmosphere below. The potential temperature jumps form preferentially at the approximate height of the canyon rims (2100 to 2300 m MSL), although they are sometimes found somewhat above or below these levels. A series of soundings taken on 22 January 1990 (Fig. 10) illustrates the persistence of such jumps. In this case, a jump of about 6 K over a height interval of 200–300 m persisted at the level of the south rim for the entire day, while the stability in the canyon below remained near neutral.

The potential temperature jumps noted in Figs. 3–5 were observed in morning and afternoon soundings on individual days of the WVS experiment. Figure 11 shows a broader sampling of potential temperature jumps that occurred above Phantom Ranch at different times of day during the experimental period. The jumps will have important air pollution implications for the Grand Canyon because their high stability decreases the vertical interchange of air and pollution between the air above and below the jump. Air within the canyon below the jump will generally be well mixed because of the weak stability within the canyon. When the canyon air is polluted, the jump will cap the canyon pollution layer. On the other hand, if the air above the jump is polluted, it will flow over the canyon and remain isolated from the canyon atmosphere. The elevation of the base of the jump is an important air pollution dispersion parameter. If the base is below the south rim, the canyon air will remain trapped within the canyon; if the base is above the south rim, air can be carried into or out of the canyon through the elevation interval between the south rim and the base of the temperature jump. Because of the air pollution implications of the jumps, it is important to determine the physical processes responsible for their formation so that one can determine when they are likely to form.

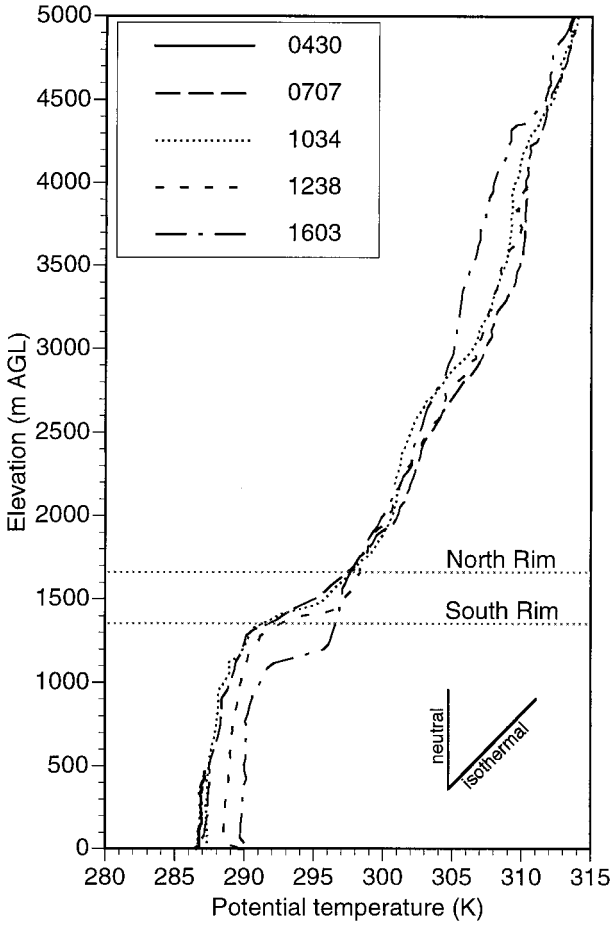

FIG. 10. Sequential tethered balloon and airsonde potential temperature profiles at Phantom Ranch during the daytime of 22 January 1990. Times indicated are in MST.

Figure 12 depicts schematically four processes that can modify temperature soundings to produce potential temperature jumps at the tops of canyons. These processes include (a) warming of the air above the canyon by large-scale warm air advection, (b) cooling of the air inside the canyon, (c) descent of a subsidence inversion to the rim levels, and (d) mixed layer growth within the canyon starting from a strong morning inversion profile. The last process, well known over homogeneous terrain, produces a potential temperature jump at the top of a growing convective boundary layer (e.g., Stull 1988).

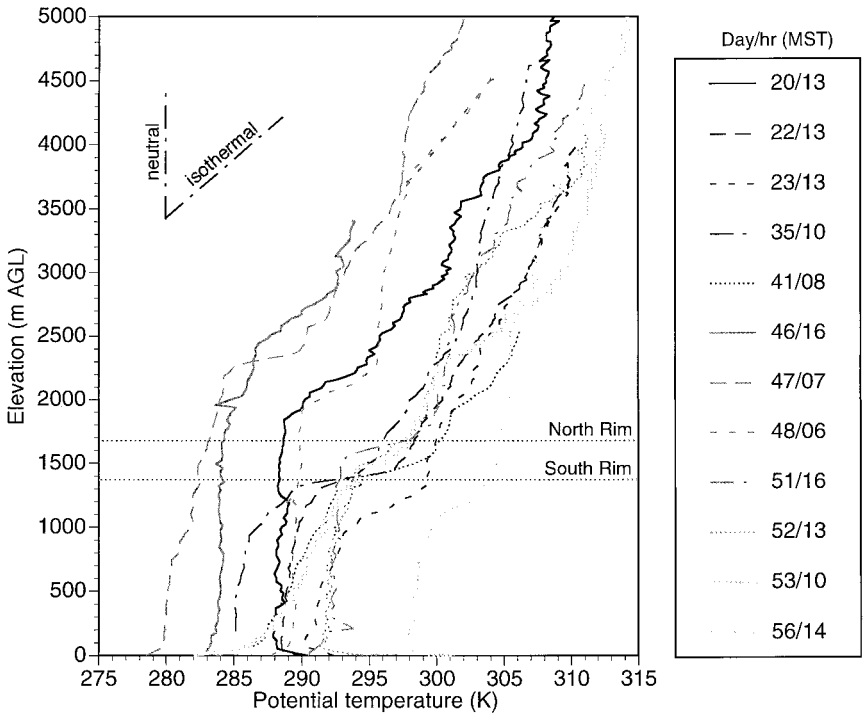

FIG. 11. Selected Phantom Ranch soundings exhibiting potential temperature jumps at elevations near the canyon rims.

Processes (c) and (d) should lead to potential temperature jumps that descend from above or grow upward from the ground, respectively. The descent of a subsidence inversion would occur at any time of the day or night, depending on synoptic-scale processes, while an inversion capping a growing convective boundary layer would occur regularly during daytime. An inspection of the canyon soundings, however, shows that the potential temperature jumps form only on certain days, occurring at any time of day and persisting over periods that can exceed 24 h. Further, the jumps were not seen to propagate consistently upward or downward to rim level, and there were no instances of potential temperature jumps in the lower two-thirds of the canyon. Rather, once the jump forms near rim level its height stays relatively constant with time. This suggests that the jumps are not generally formed by either subsidence or convective boundary layer growth.

Processes (a) and (b) call for differential heating or cooling between the canyon atmosphere and the air above the canyon. Process (b), which requires cooling inside the canyon, would occur primarily at night, but many of the potential temperature jumps occur during daytime. Therefore, analyses have been focused on process (a) to determine whether above-canyon warming associated with synoptic-scale disturbances could be responsible for the formation of the potential temperature jumps. For this analysis, we examined the time series of 70-kPa heights and temperatures at Tusayan, on the Coconino Plateau 18 km south of Phantom Ranch, for the entire experimental period (Fig. 13). The 70-kPa pressure level is typically found at 2800–3200 m MSL, about 400–800 m above the north rim. Comparison of the Tusayan 70-kPa height and temperature series with a similar series (not shown) at Winslow, Arizona, a site about 120 km southeast of Tusayan, found a good correspondence between sites, indicating that the Tusayan series represents large-scale atmospheric conditions unperturbed by local topography. The Tusayan temperature and height series in Fig. 13 show a good correlation between 70-kPa temperatures and heights, indicating that temperatures at this pressure level rise with the approach of ridges and fall with the approach of troughs. Temperature tendencies are also shown in Fig. 13, computed as the 24-h temperature difference obtained by subtracting the temperature at each observation time from the temperature at the same time on the previous day. Positive values indicate warming at the 70-kPa level over the past 24 h, while negative values indicate cooling. Since the temperature tendencies are regional, are observed above the terrain in winter, and are correlated with movement of large-scale pressure systems, the temperature tendencies are expected to be driven largely by horizontal temperature advection. The periods with strong potential temperature jumps in the Phantom Ranch soundings are indicated by the gray shading in Fig. 13. All potential temperature jumps were associated with either rising or steady temperatures and heights. Thus, we conclude that, in most cases, pronounced potential temperature jumps at the top of the

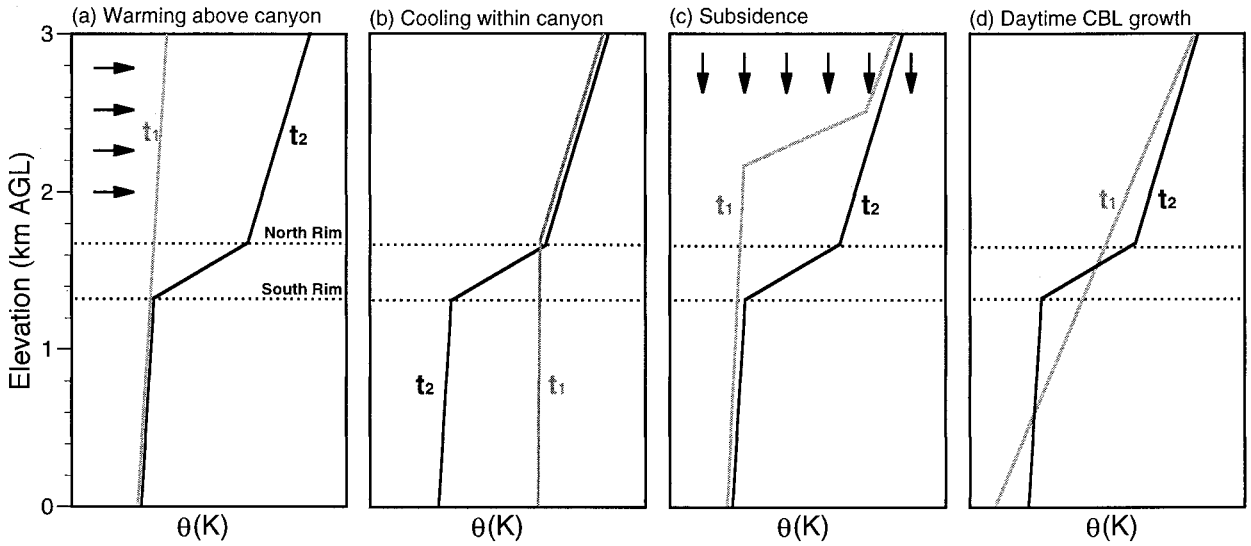

FIG. 12. Schematic diagram illustrating processes (a)–(d) that can produce potential temperature jumps at canyon rim elevations. Soundings are considered to have been made at two successive times, t_1 and t_2.

canyon are produced by large-scale warm air advection above the canyon. The warm air advection does not extend downward into the canyon because of sheltering by the surrounding higher terrain and because the flow in the canyon, rather than being parallel to the upper flow, is channeled along the canyon's axis by processes that are discussed in the following section.

6. Winds within the Grand Canyon

Wagner (1938) and Defant (1951) have described the local thermally driven wind systems that are observed in valleys all over the world. Thermally driven winds produce regular diurnal shifts in wind speed and direction, and are best developed in clear undisturbed weather conditions when winds aloft are light. The along-valley and along-slope wind systems are ubiquitous in complex terrain areas and have been reported in most of the valleys studied to date. At night, downslope and downvalley winds prevail; during daytime, upslope and upvalley winds are the general rule. Downslope and downvalley winds can persist for much of the day during short winter days, especially in snow-covered valleys or valleys where upward sensible heat fluxes are weak.

Nighttime winds, observed by tethersondes at the Phantom Ranch site, are frequently light and variable in the lowest 550 m of the canyon but are stronger and parallel to the canyon's axis in the upper two-thirds of the canyon. Nocturnal winds, while parallel to the canyon's axis, can blow either up or down the canyon, suggesting that canyon winds are channeled, rather than thermally driven. The few available soundings taken during near-clear, light-wind-aloft periods (Fig. 14), show that morning winds are from the west on some days (20 January and 6 February), but from the east on other days (28 February and 1 March). Similarly, evening winds are from the east on 20 January and 11 February, and from the west on 15 February. Thus, there is no clear diurnal variation in along-canyon wind direction. Further, canyon wind speeds are quite variable from day to day. Thus we conclude that the wintertime along-canyon wind system is not a typical thermally driven wind system.

From Fig. 1, the canyon represents a channel that connects the Colorado Plateaus Basin east of the canyon with the lower-lying Basin and Range Province west of the canyon. To evaluate the possibility that synoptic-scale pressure gradients along the canyon's axis are responsible for driving winds through this channel, we investigated the relationship between wind directions and speeds in the canyon and the synoptic-scale pressure gradient. Canyon wind speeds were determined from individual Phantom Ranch tethered balloon soundings by averaging all wind speed data points in the soundings from 1300 m MSL (i.e., 550 m above the Phantom Ranch site) to the highest point attained by the sounding. The mean speeds were given a positive sign for westerly winds that carried air up the canyon and were given a negative sign if they blew down the canyon. The horizontal pressure differences between the Basin and Range Province and the Colorado Plateaus Basin were then evaluated using upper-air soundings at Ash Fork (ASH), Arizona, and at Page (PGA), Arizona. During the WVS experiment, procedures were established and followed at the WVS upper-air sounding sites to intercompare and calibrate aneroid barometers, and to use these intercomparisons to set an accurate surface pressure before the launch of each WVS sonde (C. G. Lindsey 1995, personal communication). The horizontal pressure gradient between the Basin and Range Province and Colorado Plateaus Basin was determined by com-

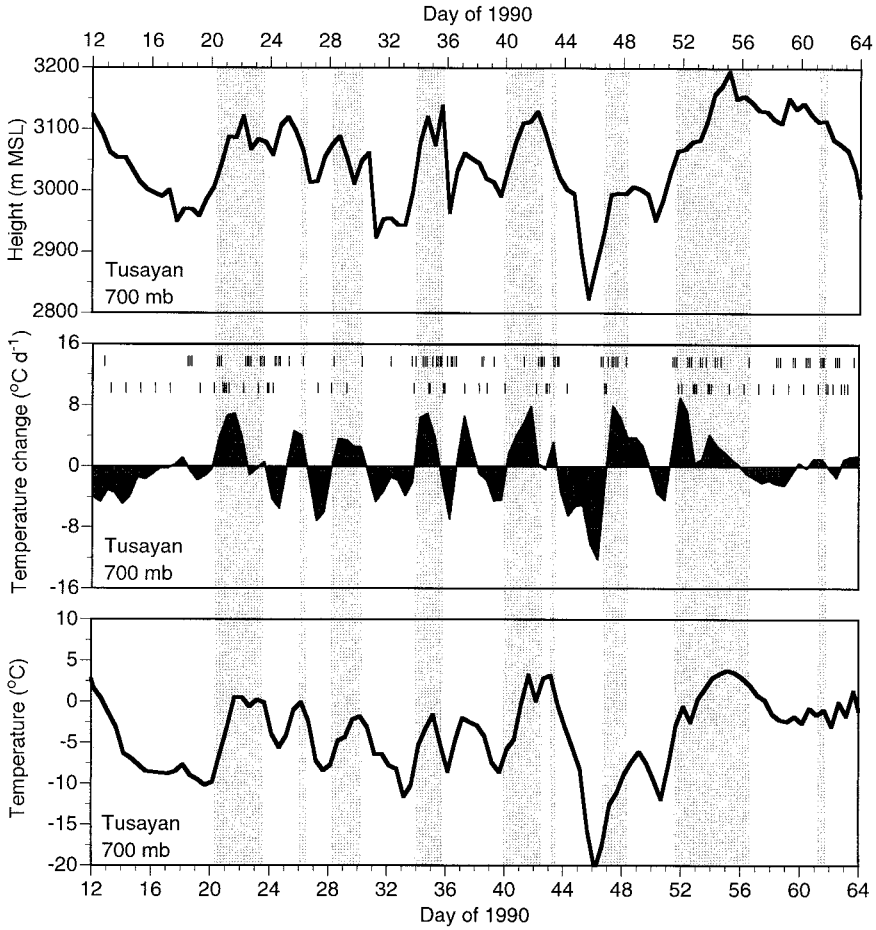

FIG. 13. Heights, temperatures, and 24-h temperature differences at the 70-kPa pressure level above Tusayan, Arizona. Temperature differences were calculated by subtracting the temperature value at a specific time from the temperature value at the same time on the previous day. The vertical strips of gray shading indicate periods when potential temperature jumps were seen above the canyon. Short vertical lines in the middle of the figure indicate the times of airsonde (upper strip) and tethered balloon (lower strip) soundings. The tethered balloon soundings are often of insufficient depth to observe the potential temperature jumps.

puting the differences in the heights of the 82.5-kPa pressure surface at the two stations using upper-air soundings that were within about 3 h of the tethered balloon wind observations in the canyon. The 82.5-kPa pressure surface was chosen to represent the middle levels of the canyon atmosphere. Figure 15 shows the relationship between the PGA–ASH height differences and the canyon wind speeds. Winds in the canyon blow down-canyon when the height gradient has one sign and blow in the opposite direction when the height gradient has the opposite sign. Canyon wind speeds increase as the height (or, equivalently, pressure) differences increase. Winds in the canyon are thus driven by horizontal pressure differences along the canyon axis between the elevated Colorado Plateaus Basin and the atmosphere in the Basin and Range Province at the canyon's west end. This pressure-driven channeling of winds in a valley has been previously noted in Germany's Rhine Valley (Gross and Wippermann 1987) and in the Tennessee Valley (Whiteman and Doran 1993). It should be noted that a preliminary investigation of channeling in the Grand Canyon by Gaynor and Ping (1993), following a conference presentation of the channeling results reported here (Whiteman 1992), found no channeling effect. Their analyses, however, used the contaminated radar profiler wind data at Phantom Ranch (see section 2c).

Wind channeling within the canyon has a number of important air pollution transport implications, since pollutant-laden air can be advected into the canyon from either the east or west end depending on the along-valley component of the synoptic-scale pressure gradient. Thus, when a low pressure system approaches the canyon from the west, or when a high pressure builds east of the canyon, air and pollutants will flow westward through the canyon from the Colorado Plateaus Basin.

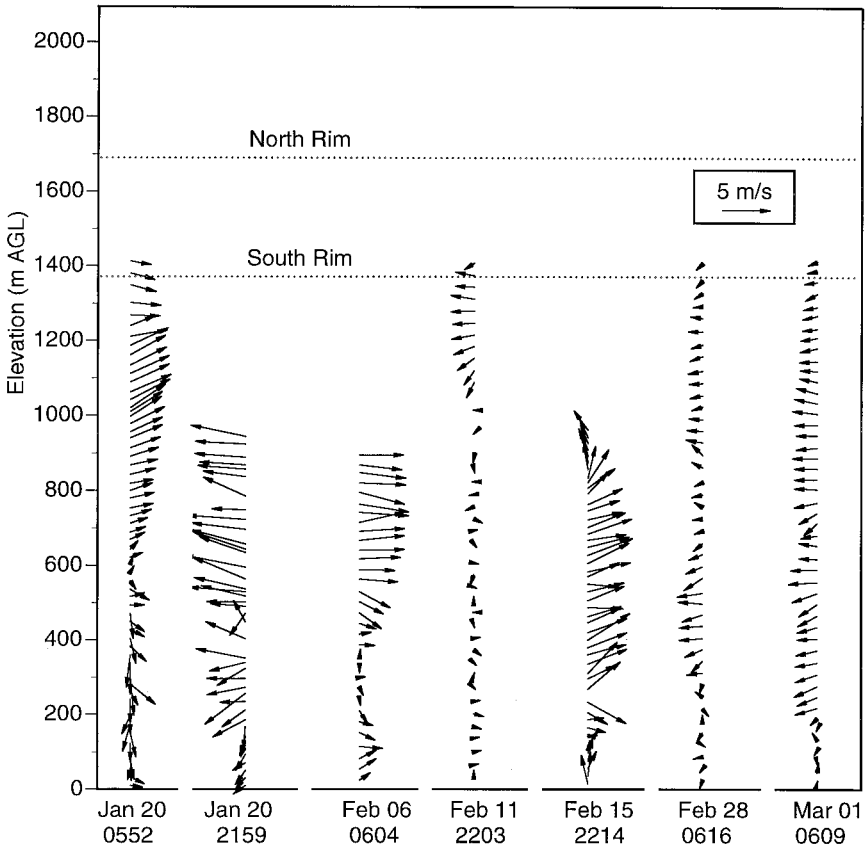

FIG. 14. Early morning and evening tethered balloon wind profiles under near-clear conditions with weak synoptic winds. Times are in MST.

Pollutants are known to build up in this basin over multiday periods (Yu and Pielke 1986; Allwine and Whiteman 1994) as pollutants from mining operations, power plants, fires, and other sources recirculate within the basin temperature inversion. Low pressures in the Colorado Plateaus Basin or high pressures west of the canyon will cause air to flow eastward through the canyon. Pollutants during these events may come from Las Vegas, the Los Angeles Basin, or from other regional sources west of the canyon (Stauffer and Seaman 1994; Green and Gebhart 1997).

The preliminary nature of the wind channeling finding must be stressed, as only 29 data points are available to relate canyon winds to synoptic-scale pressure gradients using the Phantom Ranch tethered balloon soundings and the PGA–ASH height gradients. The strength of the relationship is rather surprising in view of the nonoptimal locations of the ASH and PGA sites for measuring pressure gradients between the east and west ends of the canyon. The PGA–BUL and PGA–CAM height gradients also had some value as predictors of the canyon winds, but were not as suitable as the PGA–ASH gradients, presumably because of their poorer representativeness of the along-canyon gradients. Analyses were also performed to determine if the canyon wind direction could be determined from the 82.5-kPa height gradients between the long-term National Weather Service rawinsonde network stations at DRA (Mercury, Nevada, 36°37′N, 116°01′W, 1007 m MSL) and INW. The DRA–INW gradients (and the DRA–PGA gradients) proved to be of little value in predicting canyon winds, presumably because of the suboptimal station locations and the lack of procedures for intercomparing and setting accurate surface pressures before the National Weather Service (NWS) sondes were launched.

The strong relationship between synoptic-scale pressure gradients and winds in the canyon suggests that the canyon, and, possibly, other low-lying passes on the western edge of the Colorado Plateaus Basin, will be the conduit for channeled flows as synoptic pressure gradients vary across the region. Doppler sodar wind data collected in the WVS experiment at Fredonia, Arizona, 55 km southwest of Fredonia Pass, appear to support this view. The winds over Fredonia (not shown) are bidirectional, blowing from either the northeast or southwest, and do not appear to be predominantly diurnally forced. In winter, winds above the region are most often from the southwest. These climatologically favored winds are produced when low (high) pressure occurs to the northwest (southeast) of the canyon. In

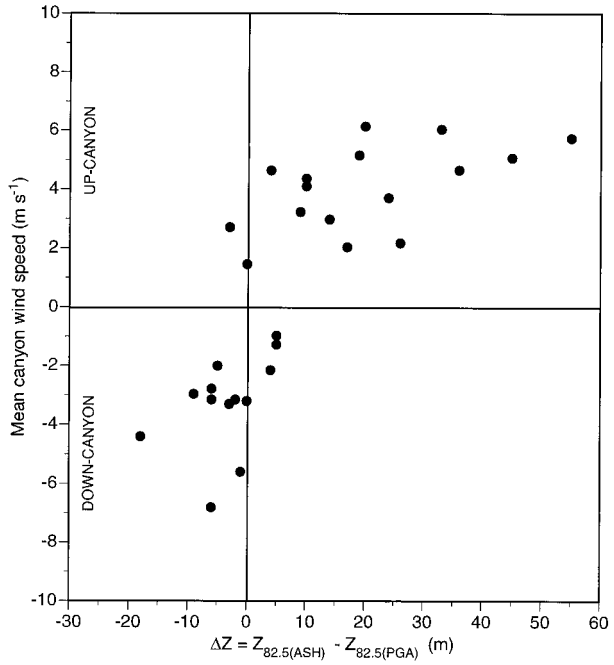

FIG. 15. Plot of the mean Grand Canyon wind speed vs the height difference at the 82.5-kPa pressure surface between Ash Fork and Page, Arizona. Up-valley flows are positive; down-valley flows are negative. Wind speeds were computed between the 550 m level above Phantom Ranch (i.e., 1300 m MSL) and the maximum height attained by the tethered balloon.

moist conditions the pressure-driven flows may produce clouds as air is carried over the passes or converges into the narrow passages.

7. Summary and conclusions

Wintertime soundings from a site on the floor of the Grand Canyon were analyzed to investigate the vertical temperature and wind structure and to determine how the atmospheric boundary layer structure evolves diurnally within the canyon. Soundings were made both night and day at irregular intervals during a 7-week period. Analyses show that the canyon's vertical temperature structure and its evolution differ from that of other Rocky Mountain valleys and from boundary layers over homogeneous terrain. Also, in contrast to other Rocky Mountain valleys, winds in the canyon are driven by synoptic-scale pressure gradients rather than exhibiting the typical thermally forced diurnal valley wind systems. Further, unusual temperature jumps often seen at the top of the canyon at the levels of the north and south rims are produced primarily by warm air advection above the canyon.

Most Rocky Mountain valleys develop nighttime temperature inversions as stable boundary layers grow upward from the valley floor. These inversions are strongest in winter during clear undisturbed nights when snow cover is present. In these valleys, following sunrise, the nighttime stable boundary layer is destroyed as a convective boundary layer grows upward from the valley floor. Winter observations in the Grand Canyon, however, show that the canyon atmosphere maintains a weak stability both day and night, rarely forming temperature inversions. The canyon atmosphere typically exhibits near-neutral to isothermal temperature gradients (i.e., $0 < d\theta/dz < 0.098$ K m^{-1}) to elevations near the canyon's rims. Daytime stability is usually close to neutral, while nighttime stability is usually between neutral and isothermal. Canyon stabilities are strongest (approaching isothermal) near the time of sunrise following clear nights. The diurnal evolution of the temperature structure is characterized by more or less uniform warming and cooling throughout the entire canyon depth or by nighttime stabilization and daytime destabilization, rather than by the upward growth of convective boundary layers or stable layers from the canyon floor.

While the weak stability and the mode of temperature structure evolution in the canyon differ from other Rocky Mountain valleys, the diurnal change in heat storage in the Grand Canyon is actually somewhat higher than in other valleys, but the cooling and heating are distributed through a deeper layer in the canyon. It is this deep distribution of the cooling that appears to be responsible for the weak nighttime stabilities. The deep distribution of the cooling is neither caused by stronger along-valley winds (and associated turbulence) in the Grand Canyon than in other valleys nor by radiative effects caused by cloudiness since the profiles exhibit only slight stability even on clear nights when along-canyon winds are weak.

A variety of physical mechanisms that could lead to the observed deep, weak-stability layers and their evolution in the absence of growing convective or stable boundary layers have been examined. The data are sufficient to reject some of the postulated physical mechanisms. It appears likely, however, that several mechanisms may act in concert to produce the observations. We speculate that downward convection of cold air drained off the snow-covered Kaibab Plateau north of the canyon and the mixing of this air horizontally across the canyon play an important role in destabilizing the canyon atmosphere during nighttime. Visual evidence from a prescribed fire on the Kaibab Plateau appears to support this mechanism. Vertical gradients of radiative flux divergence in the canyon also act to destabilize the nighttime canyon atmosphere. During daytime, convection caused by intense insolation on the south-facing slope of the canyon, combined with continued drainage of cold air into the top of the canyon from the Kaibab Plateau destabilize the canyon atmosphere.

The weak daytime and nighttime stabilities in the canyon will promote vertical and horizontal mixing of air pollution (as well as moisture and other scalars) within the canyon. The absence of growing stable and convective boundary layers suggests that plume dispersion associated with these boundary layer structures (e.g.,

fanning, fumigation, lofting, etc.) will be less important in the Grand Canyon than in other valleys or over flat terrain.

On many days, temperature jumps (typically jumps of 5 K over a depth of several hundred meters) are found to occur above the canyon at or near the level of the canyon's rims, resembling those found at the tops of growing convective boundary layers. These jumps, however, arise from a different mechanism, as they persist during both day and night, may last for more than 24 h, and form at elevations near the canyon rim rather than descending from above or growing upward from the canyon floor. These temperature jumps are caused primarily by large-scale warm air advection above the canyon rim levels. They provide an effective lid to the canyon atmosphere when they are present at or below the level of the south rim, keeping the well-mixed air within the canyon from mixing with the air aloft. Pollutants can remain trapped in the canyon for several days during the warm air advection episodes that precede the arrival of slow-moving synoptic-scale ridges, degrading canyon visibility and increasing pollutant burdens in the canyon. The height of the base of the temperature jump is expected to be an important parameter affecting air pollution dispersion in the canyon, as clean or polluted air can enter or leave the canyon by flowing over the south rim when the base of the jump is above the south rim but below the higher north rim.

Winds are often light and variable in the lowest 550 m of the canyon. Above this height, the canyon winds, while channeled along the valley's axis, are not diurnal, thermally driven up-valley/down-valley winds. Rather, the channeled winds act to equalize pressure differences that develop between air in the Colorado Plateaus Basin to the east of the canyon and air in the Great Basin west of the canyon. In wintertime, the pressure differences that drive these flows are predominantly synoptic in origin and wind direction within the canyon is determined by the along-canyon component of the synoptic-scale pressure gradient, which varies as high- and low-pressure centers move across the southwest. Pollutants can thus be advected into the canyon from either end. Since different types and strengths of regional pollutant sources are found in the Great Basin and the Colorado Plateaus Basin west and east of the canyon, the canyon wind direction will be an important determinant of canyon pollution levels.

Because so little boundary layer structure data are available for the canyon, and because boundary layer evolution and flow direction within the canyon, and temperature jumps above the canyon, have important air pollution implications, we suggest that more comprehensive meteorological field studies be conducted in the Grand Canyon in the future. These studies would be most effective if they were supported by a strong numerical modeling component. Previous research has emphasized the large-scale transport of air pollutants across the southwest toward the Grand Canyon, but there have been few investigations of the interactions between these large-scale flows and local-scale processes within the canyon that ultimately affect canyon air quality. Experiments in other seasons may be useful for refining and testing hypotheses regarding boundary layer evolution in the canyon.

Acknowledgments. The data used in our analyses were collected by participants of the Winter Visibility Study and funded by Arizona's Salt River Project (SRP). Prem Bhardwaja of SRP was the program manager. Data within the canyon were collected by the National Oceanic and Atmospheric Administration's Environmental Technology Laboratory. The analyses reported here benefited from joint planning, suggestions, and reviews from the WVS meteorological analyst team, including W. D. Neff, R. Banta, D. Wolfe, D. Ruffieux, and C. Russell at NOAA/ETL, R. K. Hauser at California State University, Chico, C. G. Lindsey at Sonoma Technology, Inc., and P. Ostapuk, J. Sutherland, and J. A. Skindlov at SRP. At Pacific Northwest National Laboratory, K. J. Allwine assisted with data processing, and J. C. Doran and J. D. Fast provided useful reviews of the manuscript.

Research was supported by the Salt River Project as part of their Winter Visibility Study and by the U.S. Department of Energy (DOE) Environmental Sciences Division under Contract DE-AC06-76RLO 1830 at Pacific Northwest National Laboratory as part of DOE's Atmospheric Studies in Complex Terrain program. Pacific Northwest National Laboratory is operated for the DOE by Battelle Memorial Institute.

REFERENCES

Allwine, K. J., and C. D. Whiteman, 1994: Single-station integral measures of atmospheric stagnation, recirculation and ventilation. *Atmos. Environ.,* **28,** 713–721.

Arritt, R. W., 1985: Numerical studies of thermally and mechanically forced circulations over complex terrain. Report prepared for National Park Service, by Cooperative Institute for Research in the Atmosphere, Fort Collins, CO, 201 pp. [Available from National Park Service, Denver, CO 80225.]

Atkinson, B. W., 1995: Orography and stability effects on valley-side drainage flows. *Bound.-Layer Meteor.,* **75,** 403–428.

Banta, R. M., L. D. Olivier, and W. D. Neff, 1991: Flow in the Grand Canyon and other valleys as revealed by Doppler lidar. Preprints, *Seventh Conf. on Applications of Air Pollution Meteorology,* New Orleans, LA, Amer. Meteor. Soc., J210–J213.

——, and Coauthors, 1999: Wind-flow patterns in the Grand Canyon as revealed by Doppler lidar. *J. Appl. Meteor.,* **38,** 1069–1083.

Davis, R. E., and D. A. Gay, 1993: A synoptic climatological analysis of air quality in the Grand Canyon National Park. *Atmos. Environ.,* **27A,** 713–727.

Defant, F., 1951: Local winds. *Compendium of Meteorology,* T. F. Malone, Ed., Amer. Meteor. Soc., 655–672.

Doran, J. C., T. W. Horst, and C. D. Whiteman, 1990: The development and structure of nocturnal slope winds in a simple valley. *Bound.-Layer Meteor.,* **52,** 41–68.

Gaynor, J. E., and R. M. Banta, 1991: Relation between cross-canyon circulations and vertical mixing into the Grand Canyon. Preprints, *Seventh Conf. on Applications of Air Pollution Meteorology,* New Orleans, LA, Amer. Meteor. Soc., 384–387.

——, and Y. J. Ping, 1993: Wind patterns in Northwestern Arizona

measured with wind profilers and implications to air pollution in Grand Canyon National Park. *Proc. AWMA 86th Annual Meeting,* Denver, CO, Air and Waste Management Association, 2–14.

GCVTC, 1996: Recommendations for improving western vistas. Report of the Grand Canyon Visibility Transport Commission to the United States Environmental Protection Agency, 91 pp. [Available from the Western Governors Association, 600 17th Street, Suite 1705, South Tower, Denver, CO 80202.]

Green, M. C., and K. A. Gebhart, 1997: Clean air corridors: A geographic and meteorologic characterization. *J. Air Waste Manage. Assoc.,* **47,** 403–410.

Gross, G., and F. Wippermann, 1987: Channeling and countercurrent in the upper Rhine Valley: Numerical simulations. *J. Climate Appl. Meteor.,* **26,** 1293–1304.

Hamblin, W. K., and J. R. Murphy, 1980: Grand Canyon Perspectives. Brigham Young University, Geology Studies, Special Publ. 1, H and M Distributors, University Station, Provo, UT, 47 pp. [Available from Geology Department Publications, BYU, Provo, UT 84602.]

Holzworth, G. C., and R. W. Fisher, 1979: Climatological summaries of the lower few kilometers of rawinsonde observations. EPA-600/4-79-026, EPA, 141 pp. [Available from NTIS, Springfield, VA 22161.]

Lindsey, C. G., J. Chen, T. S. Dye, L. W. Richards, and D. L. Blumenthal, 1999: Meteorological processes affecting the transport of emissions from the Navajo Generating Station to Grand Canyon National Park. *J. Appl. Meteor.,* **38,** 1031–1048.

Macias, E. S., J. O. Zwicker, and W. H. White, 1981: Regional haze case studies in the southwestern U.S.: II. Source contributions. *Atmos. Environ.,* **15,** 1987–1997.

Malm, W. C., M. Pitchford, and H. K. Iyer, 1988: Design and implementation of the Winter Haze Intensive Tracer Experiment—WHITEX. *Proc. 81st Annual Meeting of the Air Pollution Control Association,* Dallas, TX, Air and Waste Management Association, 28 pp.

Mueller, P. K., D. A. Hansen, and J. G. Watson Jr., 1986: The Subregional Cooperative Electric Utility, Department of Defense, National Park Service, and EPA Study (SCENES) on Visibility: An overview. Rep. EA-4664-SR, Electric Power Research Institute, Palo Alto, CA, 63 pp. [Available from Electric Power Research Institute, 3412 Hillview Ave., Palo Alto, CA 94304-1395.]

Nappo, C. J., and K. S. Rao, 1987: A model of pure katabatic flows. *Tellus,* **39A,** 61–71.

Petkovsek, Z., 1978: Zones of convergence in local air flow in valleys and basins. Tagungsbericht, 1. Teil, 15. Internationale Tagung fuer Alpine Meteorologie, Swiss Meteorological Institute, Zurich, Grindelwald, Switzerland, 92–96.

——, and A. Hocevar, 1971: Night drainage winds. *Arch. Meteor. Geophys. Bioklimatol.,* **20A,** 353–360.

Poulos, G. S., and R. A. Pielke, 1994: A numerical analysis of Los Angeles basin pollution transport to the Grand Canyon under stably stratified southwest flow conditions. *Atmos. Environ.,* **28,** 3329–3357.

Richards, L. W., C. L. Blanchard, and D. L. Blumenthal, Eds., 1991: Navajo Generating Station Visibility Study Final Report. Rep. STI-90200-1124-FR, prepared for Salt River Project from Sonoma Technology, Inc., Santa Rosa, CA. [Available from Salt River Project, Box 52025, Phoenix, AZ 85072-2025.]

Ruffieux, D., 1992: Micrometeorology in the Grand Canyon: A Case Study. Preprints, *Sixth Conf. on Mountain Meteorology,* Portland, OR, Amer. Meteor. Soc., 156–160.

——, and C. D. Whiteman, 1991: Wintertime surface energy budget variations in the Grand Canyon region. *Proc. 84th Annual Meeting, Air and Waste Management Association,* Vancouver, BC, Canada, AWMA, 14 pp.

Sinclair, P. C., and R. E. Dattore, 1987: Air Motion and Thermodynamic Structure of the Grand Canyon Atmosphere. Rep. NA81RAH00001, Department of Atmospheric Science, Colorado State University Report to National Oceanic and Atmospheric Administration, Environmental Research Laboratory, Boulder, CO, 160 pp. [Available from NOAA/ERL, Boulder, CO 80303.]

Start, G. E., C. R. Dickson, and L. L. Wendell, 1975: Diffusion in a canyon within rough mountainous terrain. *J. Appl. Meteor.,* **14,** 333–346.

Stauffer, D. R., and N. L. Seaman, 1994: Multiscale four-dimensional data assimilation. *J. Appl. Meteor.,* **33,** 416–434.

Stearns, L. P., 1987: Aspects of the local circulation at the Grand Canyon during the fall season. *J. Climate Appl. Meteor.,* **26,** 1392–1400.

Stull, R. B., 1988: *An Introduction to Boundary Layer Meteorology.* Kluwer Academic Publishers, 666 pp.

Trijonis, J., 1979: Visibility in the Southwest—An exploration of the historical data base. *Atmos. Environ.,* **13,** 833–843.

Wagner, A., 1938: Theorie und Beobachtung der periodischen Gebirgswinde (Theory and observation of periodic mountain winds). *Gerlands Beitr. Geophys.,* **52,** 408–449. English translation by C. D. Whiteman, and E. Dreiseitl, 1984: Alpine Meteorology: Translations of Classic Contributions by A. Wagner, E. Ekhart and F. Defant. PNL-5141 / ASCOT-84-3, Pacific Northwest Laboratory, Richland, WA, 121 pp.

Watson, J. G., M. Green, and T. E. Hoffer, 1993: Project MOHAVE Data Analysis Plan. *Proc. 86th Annual Meeting,* Denver, CO, Air and Waste Management Association, 16 pp.

Whiteman, C. D., 1980: Breakup of temperature inversions in Colorado mountain valleys. Ph.D. dissertation, Atmospheric Science Paper 328, Colorado State University, 250 pp. [Available from UMI Company, 300 N. Zeeb Rd., P.O. Box 1346, Ann Arbor, MI 48106.]

——, 1982: Breakup of temperature inversions in deep mountain valleys: Part I. Observations. *J. Appl. Meteor.,* **21,** 270–289.

——, 1986: Temperature inversion buildup in Colorado's Eagle Valley. *Meteor. Atmos. Phys.,* **35,** 220–226.

——, 1992: Wintertime meteorology of the Grand Canyon region. Preprints, *Sixth Conf. on Mountain Meteorology,* Portland, OR, Amer. Meteor. Soc., 144–150.

——, and K. J. Allwine, 1986: Extraterrestrial solar radiation on inclined surfaces. *Environ. Software,* **1,** 164–169.

——, and J. C. Doran, 1993: The relationship between overlying synoptic-scale flows and winds within a valley. *J. Appl. Meteor.,* **32,** 1669–1682.

——, N. S. Laulainen, G. A. Sehmel, and J. M. Thorp, 1981: Green River Air Quality Model Development: Meteorological Data—August 1980 Field Study in the Piceance Creek Basin Oil Shale Resources Area. EPA-600/S7-82-047, 172 pp. [NTIS PB-82-258 6091.]

——, T. B. McKee, and J. C. Doran, 1996: Boundary Layer Evolution within a Canyonland Basin. Part I. Mass, Heat, and Moisture Budgets from Observations. *J. Appl. Meteor.,* **35,** 2145–2161.

——, X. Bian, and J. L. Sutherland, 1999a: Wintertime surface wind patterns in the Colorado River valley. *J. Appl. Meteor.,* **38,** 1118–1130.

——, ——, and S. Zhong, 1999b: Wintertime evolution of the temperature inversion in the Colorado Plateau Basin. *J. Appl. Meteor.,* **38,** 1103–1117.

Yu, C.-H., and R. A. Pielke, 1986: Mesoscale air quality under stagnant synoptic cold season conditions in the Lake Powell area. *Atmos. Environ.,* **20,** 1751–1762.